Channel Estimation for OFDM Systems with Multiple Transmit Antennas by Filtering in Time and Frequency

Gunther Auer
DoCoMo Communications Laboratories Europe GmbH,
Landsberger Straße 312, 80687 München, Germany.
Email: auer@docomolab-euro.com

***Abstract*— We address pilot-symbol aided channel estimation (PACE) for orthogonal frequency division multiplexing (OFDM) based systems, with multiple transmit antennas. An approach is presented which estimates and separates N_T superimposed signals, corresponding to N_T transmit antennas, in two dimensions. More specifically, we extend the concept of using two one dimensional (1D) estimators, instead of a truly two dimensional (2D) estimator to MIMO-OFDM systems, by dividing the estimation as well as the separation task into two stages. To this end, each estimator only separates a subset of the N_T superimposed signals, together with smoothing and interpolation in the respective dimension. Design rules for the optimization of the proposed 2×1D estimator are established, dependent on the performance, computational complexity, induced delay, and overhead due to pilot symbols.**

I. Introduction

Multi-carrier modulation, in particular OFDM [1], has been successfully applied to a wide variety of digital communications systems over the past several years. For the transmission of large data rates its superior performance in transmission through dispersive channels is a major advantage.

Transmitting a radio signal over a multipath fading channel, the received signal will have unknown amplitude and phase variations. In order to coherently detect the received signal, accurate channel estimation is essential. For multi-carrier systems the received signal after multi-carrier demodulation is typically correlated in two dimensions, in time and frequency. By periodically inserting pilots in the time-frequency grid, such that the 2D sampling theorem is satisfied, the channel response can be reconstructed by exploiting the correlation of the received signal in time and frequency. For the single transmit antenna case, 2D filtering algorithms have been proposed for PACE, based on 2D Wiener filter interpolation. Unfortunately, such a 2D estimator structure may be too complex for practical implementation. To reduce the complexity, two cascaded 1D estimators in time and frequency may be used instead, termed two times one-dimensional (2×1D) PACE [2].

Systems employing multiple transmit and receive antennas, known as multiple input multiple output (MIMO) systems, can be used with OFDM to improve the communication capacity and quality of mobile radio systems. If different signals are transmitted form different transmit antennas simultaneously, e.g. for space-time coded OFDM, the received signal is the superposition of these signals, which implies new challenges for channel estimation.

The majority of the publications about MIMO-OFDM channel estimation were limited to 1D channel estimation having 2 transmit antennas [3–5]. We aim to extend the concept of 2×1D PACE to OFDM systems with $N_T > 2$ transmit antennas. By doing so reliable channel estimation for a larger number of transmit antennas, even at high Doppler frequencies, can be provided. The basic idea of our approach is to divide the estimation and separation of the N_T superimposed signals into two stages, in the way that we first separate a subset of the N_T signals together with channel estimation in the first dimension. In the second stage we separate the remaining superimposed signals for each of the outputs of the first stage, together with channel estimation in the second dimension, to yield the desired estimate of the frequency response. With this framework known one dimensional MIMO-OFDM channel estimation schemes can be used.

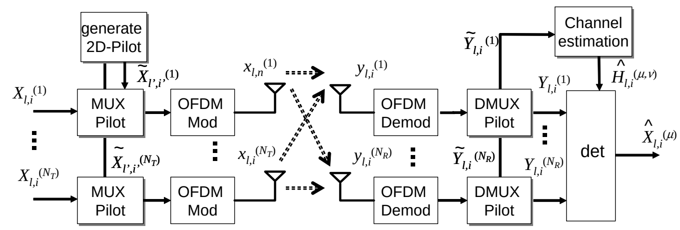

Fig. 1. Block diagram of the OFDM system with N_T transmit antennas.

By adopting the subset dimension to a given scenario, such as the channel characteristics, the OFDM system parameters, and selection of the pilot grid, this approach offers an additional degree of freedom to optimize the channel estimator. We show that the performance of the proposed 2×1D estimator is invariant on whether estimation in frequency or time direction is performed first. The computational complexity, on the other hand, is not independent on the ordering.

The remainder of this paper is structured as follows: after a brief discription of the system model in section II, the concept of 2×1D PACE will be applied to a MIMO-OFDM system in section III, and some results for a OFDM system with multiple transmit antennas are presented in section IV.

II. System and Channel Model

For the considered MIMO-OFDM system with N_T transmit and N_R receive antennas, one OFDM modulator is employed on each transmit antenna, as illustrated in Fig. 1. For OFDM the signal stream is divided into N_c parallel substreams, typical for any multi-carrier modulation scheme. The i^{th} substream, termed subcarrier, of the ℓ^{th} symbol block, named OFDM symbol, transmitted from antenna μ, is denoted by $X^{(\mu)}_{\ell,i}$. An inverse DFT with $N_{FFT} \geq N_c$ points is performed on each block, and subsequently a guard interval (GI) having N_{GI} samples is inserted, in the form of a cyclic prefix. Subsequently the signal is transmitted over a multipath fading channel. At the receiver of the ν^{th} antenna branch, the guard interval is removed and an DFT on the received block of signal samples is performed, to obtain the output of the OFDM demodulation $Y_{\ell,i}^{(\nu)}$. The received signal consists of superimposed signals from N_T transmit antennas. We assume the cyclic prefix to yield perfect orthogonality. Furthermore, the channel is assumed to be constant over one OFDM symbol. Then, the received signal after OFDM demodulation is given by

$$Y_{\ell,i}^{(\nu)} \;=\; \sum_{\mu=1}^{N_T} X_{\ell,i}^{(\mu)}\, H_{\ell,i}^{(\mu,\,\nu)} + N_{\ell,i}^{(\nu)} \tag{1}$$

where $X_{\ell,i}^{(\mu)}$, $H_{\ell,i}^{(\mu,\,\nu)}$, and $N_{\ell,i}^{(\nu)}$, denote the transmitted symbol, the channel state informaion (CSI), and additive white Gaussian noise (AWGN) with zero mean and variance N_0.

We consider a time-variant, frequency selective, Rayleigh fading channel, modeled by a tapped delay line with Q_0 non-zero taps [6]. The CSI of (1), is the Fourier transform of the channel impulse response, transmitted from antenna μ to receive antenna ν, described by

$$H_{\ell,i}^{(\mu,\,\nu)} = \sum_{q=1}^{Q_0} h_{\ell,q}^{(\mu,\,\nu)}\, e^{-j2\pi\, \tau_q^{(\mu,\,\nu)}\, i/T} \tag{2}$$

where $1/T$ is the subcarrier spacing The channel of the q^{th} tap, $h_{\ell,q}^{(\mu,\,\nu)}$, impinging with time delay $\tau_q^{(\mu,\,\nu)}$, is a wide sense stationary (WSS), complex Gaussian random variable with zero mean. All channel taps and all antennas are assumed to be mutually uncorrelated. Due to the motion of the vehicle $h_{\ell,q}^{(\mu,\,\nu)}$ will be time-variant caused by the Doppler effect, being band-limited by the maximum Doppler frequency ν_{max}.

Note that the channel estimation blocks of all N_R receive antennas are independent, provided that all receive antennas are mutually uncorrelated. Thus, the index denoting the receive antenna, ν, will be dropped in the following.

III. Principle of Pilot Symbol Aided Channel Estimation for OFDM-based MIMO Systems

Pilot aided channel estimation (PACE), based on periodically inserting known symbols, termed *pilot symbols*, in the transmitted data sequence, was first introduced for single carrier systems and required a flat-fading channel [7]. If the spacing of the pilots is sufficiently close to satisfy the sampling theorem, channel estimation and interpolation for the entire data sequence is possible. Extending PACE to multi-carrier systems the fading fluctuations are in two dimensions, in time and frequency. In order to satisfy the 2D sampling theorem, the pilot symbols are scattered throughout the time-frequency grid, yielding a 2D pilot grid. We employ a pilot grid with equidistant pilot spacing of D_f and D_t in frequency and time.

To describe PACE it is useful to define a subset of the received signal sequence containing only the pilots,[1] $\{\tilde{X}_{\tilde{\ell},\tilde{i}}^{(\mu)}\} = \{X_{\ell,i}^{(\mu)}\}$, with $\ell = \tilde{\ell} D_t$ and $i = \tilde{i} D_f$.

A. Principle of 2×1D-PACE

For 2×1D-PACE the correlation function of the channel can be factored into a time and frequency correlation function, which enables a cascaded channel estimator, consisting of two 1D estimators. The basic idea of 2×1D-PACE is illustrated in Fig. 2. Channel estimation in the 1st dimenstion (in Fig. 2 the frequency direction), at OFDM symbols $\ell = \tilde{\ell} D_t$, yields tentative estimates for all subcarriers of that OFDM symbol. The second step is to use these tentative estimates as new pilots, in order to estimate the channel for the entire frame [2]. It was demonstrated in [2], that 2×1D-PACE is significantly less complex to implement with respect to optimum 2D channel estimation, while there is little degradation in performance.

[1]As a general convention, variables describing pilot symbols will be marked with a ˜ in the following.

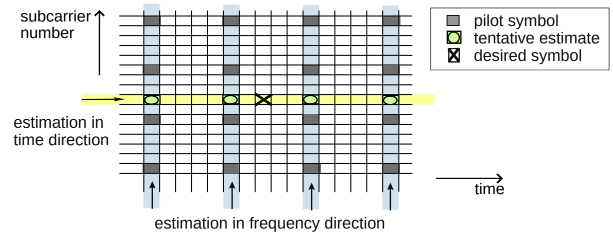

Fig. 2. Principle of 2×1D pilot aided channel estimation (PACE).

Generally, it is of great computational complexity to use all available pilots. Instead a 2D window of size $M_f \times M_t$ can be slid over the whole grid, with M_f and M_t being smaller than the number of available pilots. We assume a broadcasting scenario, that is the signal is transmitted continously.

Either channel estimation in frequency or time direction may be performed first, which will be referred to as 2×1D-PACE type I and type II, respecively.

B. Extension of 2×1D-PACE to MIMO-OFDM systems

In the following we extend 2×1D-PACE to a MIMO-OFDM system. Let us divide the set of N_T transmit antennas into N_{Tf} subsets $\mathcal{A}_{\mu_f} \subset \mathcal{A}$, each subset containing N_{Tt} signals, such that $N_T = N_{Tf} N_{Tt}$. In order to extend the pilot sequence design for an MIMO-OFDM system, we choose a set of pilot sequences which can be expressed in the product form

$$\begin{aligned}\tilde{X}_{\tilde{\ell},\tilde{i}}^{(\mu)} \;&=\; \tilde{X}_{f_{\tilde{i}}}^{(\mu_f)} \cdot \tilde{X}_{t_{\tilde{\ell}}}^{(\mu_t)},\;\; \mu = \mu_t + N_{Tt}\cdot(\mu_f - 1) \\ &\qquad\qquad 1 \le \mu_f \le N_{Tf}\;,\;\; 1 \le \mu_t \le N_{Tt}\end{aligned} \tag{3}$$

where $\tilde{X}_{f_{\tilde{i}}}^{(\mu_f)}$ and $\tilde{X}_{t_{\tilde{\ell}}}^{(\mu_t)}$ are the pilot symbols for the frequency and time direction respectively. It is important to note that the pilot symbols in frequency $\tilde{X}_{f_{\tilde{i}}}^{(\mu_f)}$ only depend on the subcarrier index $\tilde{i}$, while the pilot symbols in time $\tilde{X}_{t_{\tilde{\ell}}}^{(\mu_t)}$ only depend on OFDM symbol $\tilde{\ell}$. The pilot sequences are generally chosen from orthogonal designs. We use Walsh sequences in both frequency and time direction.

Substituting the proposed 2D pilot sequence of (3) into the sequence of received pilots, $\tilde{Y}_{\tilde{\ell},\tilde{i}} = \sum_{\mu=1}^{N_T} \tilde{X}_{\tilde{\ell},\tilde{i}}^{(\mu)} \tilde{H}_{\tilde{\ell},\tilde{i}}^{(\mu)} + \tilde{N}_{\tilde{\ell},\tilde{i}}$, the following is obtained

$$\tilde{Y}_{\tilde{\ell},\tilde{i}} = \sum_{\mu_f=1}^{N_{Tf}} \tilde{X}_{f_{\tilde{i}}}^{(\mu_f)} \tilde{Z}_{f_{\tilde{\ell},\tilde{i}}}^{(\mu_f)} + \tilde{N}_{\tilde{\ell},\tilde{i}} = \sum_{\mu_t=1}^{N_{Tt}} \tilde{X}_{t_{\tilde{i}}}^{(\mu_t)} \tilde{Z}_{t_{\tilde{\ell},\tilde{i}}}^{(\mu_t)} + \tilde{N}_{\tilde{\ell},\tilde{i}} \tag{4}$$

with

$$\tilde{Z}_{f_{\tilde{\ell},\tilde{i}}}^{(\mu_f)} \triangleq \sum_{\mu_t=1}^{N_{Tt}} \tilde{X}_{t_{\tilde{\ell}}}^{(\mu_t)} \tilde{H}_{\tilde{\ell},\tilde{i}}^{(\mu)} \quad \text{and} \quad \tilde{Z}_{t_{\tilde{\ell},\tilde{i}}}^{(\mu_t)} \triangleq \sum_{\mu_f=1}^{N_{Tf}} \tilde{X}_{f_{\tilde{i}}}^{(\mu_f)} \tilde{H}_{\tilde{\ell},\tilde{i}}^{(\mu)} \tag{5}$$

where $\mu = \mu_t + N_{Tt}\cdot(\mu_f - 1)$. Since $\tilde{X}_{t_{\tilde{\ell}}}^{(\mu_t)}$ in (3) is constant with respect to the subcarrier index $\tilde{i}$, $\tilde{Z}_{f_{\tilde{\ell},\tilde{i}}}^{(\mu_f)}$ is a superposition of N_{Tt} waveforms each multiplied with a constant phase term. So, $\tilde{Z}_{f_{\tilde{\ell},\tilde{i}}}^{(\mu_f)}$ in (5) may be viewed as the resulting channel response of subset μ_f in frequency direction. Accordingly, $\tilde{Z}_{t_{\tilde{\ell},\tilde{i}}}^{(\mu_t)}$ may be viewed as the resulting channel response of

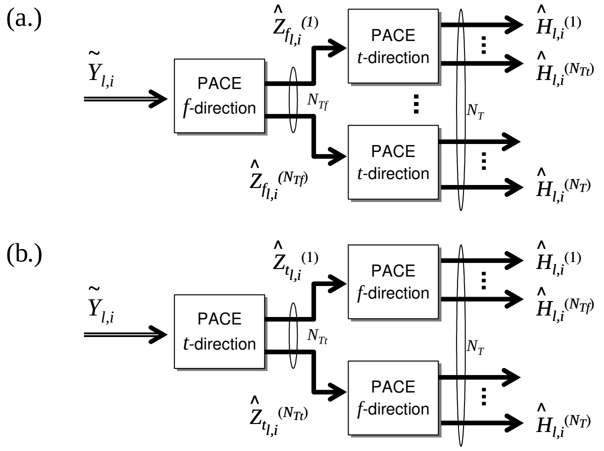

Fig. 3. Principle of 2×1D PACE type I (a.) and type II (b.), for OFDM systems with multiple transmit antennas.

subset μ_t in time direction, since $\tilde{X}^{(\mu_f)}_{f_{\tilde{i}}}$ is constant with respect to the time index $\tilde{\ell}$.

1) Comparison between 2×1D-PACE type I and type II: For 2×1D-PACE type I the task of the 1st stage is to separate the N_{Tf} subsets, as well as to estimate and interpolate the channel in frequency direction. The outputs of the 1st stage are subsequently used as inputs for the 2nd stage. In the 2nd stage we estimate the channel in time direction to separate the remaining N_{Tt} signals per subset to yield in total N_T estimates of the frequency response $\widehat{H}^{(\mu)}_{\ell,i}$. Fig. 3.a illustrates the basic idea of 2×1D-PACE type I.

The estimator for 2×1D-PACE type I can be expressed as

$$\widehat{H}^{(\mu)}_{\ell,i} = \sum_{n=1}^{M_t} W''^{(\mu)}_n(\Delta\ell) \sum_{m=1}^{M_f} W'^{\,(\mu_f)}_m(\Delta i)\cdot \tilde{Y}_{\tilde{\ell}-n,\tilde{i}-m} \quad (6)$$

where the FIR interpolation filter in frequency direction $\mathbf{W}'^{(\mu_f)}(\Delta i) = [W'^{(\mu_f)}_1(\Delta i),\cdots,W'^{(\mu_f)}_{M_f}(\Delta i)]$ depends on the location of the desired symbol relative to the pilot positions, $\Delta i = D_f\tilde{i} - i$. If $\widehat{Z}^{(\mu_f)}_{\tilde{\ell},i}$ is in the center of the sliding window, $\Delta i = D_f M_f/2 - (i \mod D_f)$. Only if $i < D_f\lfloor M_f/2\rfloor$ or $\tilde{i} > N_c - D_f\lfloor M_f/2\rfloor$, i.e. for subcarriers near the band edges, then $\Delta i = D_f\lfloor M_f/2\rfloor - (i \mod [D_f M_f])$.

The FIR interpolation filter in time direction $\mathbf{W}''^{(\mu)}(\Delta\ell) = [W''^{(\mu)}_1(\Delta\ell),\cdots,W''^{(\mu)}_{M_t}(\Delta\ell)]$, with filter delay $\Delta\ell = D_t\tilde{\ell} - \ell$. We employ a smoothing type filter which estimates the symbol in the center of the sliding window, so $\Delta\ell = D_t\lfloor M_t/2\rfloor - (\ell \mod D_t)$. This generally achieves the best performance [8]. However, buffering of $\Delta_\ell = \lfloor D_t(M_t/2–1)\rfloor$ OFDM symbols is required, and a corresponding time delay is induced. Thus, as a design rule the number of filter coefficients in time direction should be as small as possible.

2×1D-PACE type II is illustrated in Fig. 3.b. Now, channel estimation in the first dimension corresponds to the time direction. In the 1st stage N_{Tt} tentative estimates are produced, which are further processed in the 2nd stage to yield the desired N_T ouputs. Equation (6) can be rewritten to

$$\widehat{H}^{(\mu)}_{\ell,i} = \sum_{m=1}^{M_f} V'^{\,(\mu)}_m(\Delta i) \sum_{n=1}^{M_t} V''^{(\mu_t)}_n(\Delta\ell)\cdot \tilde{Y}_{\tilde{\ell}-n,\tilde{i}-m} \quad (7)$$

which is the estimator for 2×1D-PACE type II. It is seen that if $\mathbf{W}'^{(\mu_f)}(\Delta i) = \mathbf{V}'^{(\mu)}(\Delta i)$ and $\mathbf{W}''^{(\mu)}(\Delta\ell) = \mathbf{V}''^{(\mu_t)}(\Delta\ell)$, (6) and (7) are equivalent. In any case, the ordering of the filtering in (6) and (7) can be reversed. Hence, the performance of 2×1D-PACE type I and type II are identical as long as they employ the same estimators. The computational complexity, however, is in general not identiacal, a fact which will be ellaborated further in section III-C.2.

C. Derivation of the cascaded 1D estimators

According to (6) and (7) there are two separate 1D estimators for type I and II. Instead of deriving the four estimators separately, we define an auxilary signal for which the Wiener interpolation filter is determined. Let an auxilary signal be defined by

$$\tilde{\boldsymbol{\xi}} = \sum_{n=1}^{N} \tilde{\boldsymbol{\Upsilon}}^{(n)}\cdot\tilde{\boldsymbol{\zeta}}^{(n)} + \tilde{\boldsymbol{\eta}}\ , \quad \in \mathbb{C}^{M\times 1} \quad (8)$$

where $\tilde{\boldsymbol{\xi}}$, $\tilde{\boldsymbol{\Upsilon}}^{(n)} = \mathrm{diag}(\tilde{\mathbf{x}}^{(n)})$, $\tilde{\boldsymbol{\zeta}}^{(n)}$ and $\tilde{\boldsymbol{\eta}}$ denote the received and transmitted pilot sequence, the CSI, and the AWGN term, respectively, all of dimension M. The estimator for the m^{th} entry of $\tilde{\boldsymbol{\zeta}}^{(n)}$ is in the form $\widehat{\zeta}^{(n)}_m = \boldsymbol{\omega}^{(n)}\tilde{\boldsymbol{\xi}}$. To determine a Wiener interpolation filter for $\boldsymbol{\omega}^{(n)} = \mathbf{R}^{(n)}_{\zeta\tilde{\boldsymbol{\xi}}}\cdot\mathbf{R}^{-1}_{\tilde{\boldsymbol{\xi}}\tilde{\boldsymbol{\xi}}}$, the mean squard error (MSE) between the filtered received pilots sequence, $\widehat{\zeta}^{(n)}_m$, and the desired response, $\zeta^{(n)}_m$, is minimized. In this case knowledge about the channel statistics are required. The auto-correlation matrix of the received pilots is described by

$$\mathbf{R}_{\tilde{\boldsymbol{\xi}}\tilde{\boldsymbol{\xi}}} = E\big[\tilde{\boldsymbol{\xi}}\tilde{\boldsymbol{\xi}}^H\big] = \sum_{n=1}^{N}\tilde{\boldsymbol{\Upsilon}}^{(n)}\,E\big[\tilde{\boldsymbol{\zeta}}^{(n)}\tilde{\boldsymbol{\zeta}}^{(n)\,H}\big]\,\tilde{\boldsymbol{\Upsilon}}^{(n)\,H} + \alpha_w N_0\,\mathbf{I} \quad (9)$$

The auto-correlation matrix of AWGN is described by $N_0\,\mathbf{I}$, where $\mathbf{I}$ denotes the identity matrix. The cross-correlation vector between the received pilots and the desired response is given by

$$\mathbf{R}^{(n)}_{\zeta\tilde{\boldsymbol{\xi}}} = E\big[\zeta^{(n)}_m\tilde{\boldsymbol{\xi}}^H\big] = E\big[\zeta^{(n)}_m\tilde{\boldsymbol{\zeta}}^{(n)\,H}\big]\cdot\tilde{\boldsymbol{\Upsilon}}^{(n)\,H} \quad (10)$$

Considering 2×1D-PACE type I, channel estimation in frequency direction is performed in the 1st stage and utilizes the pilots of OFDM symbol $\tilde{\ell}D_t$, $\tilde{\mathbf{Y}}'_{\tilde{\ell},\tilde{i}} = [\tilde{Y}_{\tilde{\ell},\tilde{i}},\cdots,\tilde{Y}_{\tilde{\ell},\tilde{i}-M_f+1}]^T$. The 1st stage estimator is in the form $\widehat{Z}^{(\mu_f)}_{f_{\tilde{\ell},i}} = \mathbf{W}'^{(\mu_f)}(\Delta i)\tilde{\mathbf{Y}}'_{\tilde{\ell},\tilde{i}}$. Thus, by substituting $\tilde{\mathbf{Y}}'_{\tilde{\ell},\tilde{i}} = \tilde{\boldsymbol{\xi}}$, $\widehat{Z}^{(\mu_f)}_{f_{\tilde{\ell},i}} = \widehat{\zeta}^{(\mu_f)}_i$, with $N_{Tf} = N$, and $M_f = M$, the estimator $\mathbf{W}'^{(\mu_f)}(\Delta i) = \boldsymbol{\omega}^{(n)}$ can be determined by using (8).

For the 2nd stage, in order to estimate $\widehat{H}^{(\mu)}_{\ell,i}$, we use the tentative estimates at subcarrier i and subset μ_f, $\widehat{\mathbf{Z}}''^{\,(\mu_f)}_{\tilde{\ell},i} = [\widehat{Z}^{(\mu_f)}_{\tilde{\ell},i},\cdots,\widehat{Z}^{(\mu_f)}_{\tilde{\ell}-M_t+1,i}]$. By substituing $\widehat{\mathbf{Z}}''^{\,(\mu_f)}_{\tilde{\ell},i} = \tilde{\boldsymbol{\xi}}$ in (8), the 2nd stage estimator $\mathbf{W}''^{(\mu)}(\Delta\ell) = \boldsymbol{\omega}^{(\mu)}$ of subset $\mathcal{A}_{\mu_f}$ is obtained.

Accordingly, the estimators $\mathbf{V}'^{(\mu)}(\Delta i)$ and $\mathbf{V}''^{(\mu_t)}(\Delta\ell)$ for 2×1D-PACE type II can be obtained by adjusting (8).

It can be shown that, if the channels per transmit antenna have the same statistics, i.e. the same power delay profile and Doppler power spectrum, the estimators of type I and II are equivalent. Note that the signal to noise ratio (SNR) of the noise process seen by the 2nd stage estimator is improved due to the 1st stage filtering. This SNR improvement, α_w from (9), should be taken into account by generating the Wiener filters. However, it is seen from (6) and (7) that the channel estimate itself is independent on the ordering of filtering (frequency or time first). Hence, due to symmetry reasons the SNR enhancement should be applied to the time and frequency estimator. The quantity of the SNR improvement depends on the channel characteristics and the system parameters. Trials with variying values for the SNR enhancement suggested that $\alpha_w \approx \sqrt{(M_f + M_t)/2}$.

1) Mismatched estimator: For the Wiener filter in time and frequency described above, the auto and cross-correlation matrices at the receiver need to be estimated. Alternatively, a robust estimator with a model mismatch may be chosen [2]. That is to assume a uniform power delay profile with maximum delay, $\tau_{\max_w}$, and a rectangular Doppler power spectrum with the maximum Doppler frequency, $\nu_{\max_w}$, which are to be expected in a certain transmission scenario, i.e. worst case propagation delays and maximum expected velocity of the mobile user. In order to determine the channel estimator only $\tau_{\max_w}$, $\nu_{\max_w}$, and the highest expected SNR γ_w are required.

2) Complexity analysis: The computational complexity of the channel estimator is roughly approximated by the number of multiplication per estimated CSI per transmit antenna, $H^{(\mu)}_{\ell,i}$. For 2×1D-PACE type I, the number of real multiplications required for 1st and 2nd stage channel estimation is given by $C^{[1]}_f = 4M_f/(D_t N_{Tt})$ and $C^{[1]}_t = 2M_t$, respectively. Note, that for the 1st stage filter in frequency direction the filter coefficients are complex valued, resulting in 4 real multiplications per coefficient, while the 2nd stage coefficients are real valued which cuts the number of real multiplications per coeffient to 2. The total number of multiplications is simply the sum of $C^{[1]}_f$ and $C^{[1]}_t$, that is

$$C^{[1]} = 2 \cdot \big(2M_f/(D_t N_{Tt}) + M_t\big) \tag{11}$$

Accordingly, the number of multiplication for 2×1D-PACE type II are found to be

$$C^{[2]} = 2 \cdot \big(2M_f + M_t/(D_f N_{Tf})\big) \tag{12}$$

which is, in general, different to $C^{[1]}$ from (11). To conclude, the choice between 2×1D-PACE type I and type II is only based on the complexity not the performance.

D. MSE analysis

The MSE of an arbitrary 2D estimator $\mathbf{W}^{(\mu)}$ of dimension $1 \times M_f M_t$ can be expressed in the general form

$$\begin{aligned} E\big[\big|H^{(\mu)}_{\ell,i} - \widehat{H}^{(\mu)}_{\ell,i}\big|^2\big] &= E\big[\big|H^{(\mu)}_{\ell,i}\big|^2\big] \\ &- 2\,\mathrm{Re}\big\{\mathbf{W}^{(\mu)}\mathbf{R}^{(\mu)}_{H\tilde{\mathbf{Y}}}(\Delta\ell, \Delta i)\big\} + \mathbf{W}^{(\mu)}\mathbf{R}_{\tilde{\mathbf{Y}}\tilde{\mathbf{Y}}}\mathbf{W}^{(\mu)\,H} \end{aligned} \tag{13}$$

with $\widehat{H}^{(\mu)}_{\ell,i} = \mathbf{W}^{(\mu)}\tilde{\mathbf{Y}}_{\tilde{\ell},\tilde{i}}$. The $M_f M_t$ dimension vector

$$\tilde{\mathbf{Y}}_{\tilde{\ell},\tilde{i}} = [\tilde{Y}_{\tilde{\ell},\tilde{i}}, \cdots, \tilde{Y}_{\tilde{\ell},\tilde{i}-M_f+1}, \cdots, \tilde{Y}_{\tilde{\ell}-M_t+1,\tilde{i}-M_f+1}]^T$$

accounts for the received pilot sequence in frequency and time, and is used to determine the 2D correlation functions $\mathbf{R}_{\tilde{\mathbf{Y}}\tilde{\mathbf{Y}}}$ and $\mathbf{R}^{(\mu)}_{H\tilde{\mathbf{Y}}}(\Delta\ell, \Delta i)$. For 2×1D PACE the two 1D estimators are used, so

$$\mathbf{W}^{(\mu)} = \mathbf{W}''^{(\mu)}(\Delta\ell) \otimes \mathbf{W}'^{(\mu_f)}(\Delta i)\,, \quad \mu \in \mathcal{A}_{\mu_f} \tag{14}$$

where the $\otimes$ operator denotes the Kronecker product.

E. Selection of the pilot grid

The pilot spacing in frequency and time must satisfy the 2D sampling theorem, which requires that $D_f \tau_{max}/T \le 1$ and $\nu_{max} T_{sym} D_t \le 1/2$ [2]. With the system parameters from Table I we obtain $D_f \le 5$ and $D_t \le 38$. In [2] two times oversampling was suggested for a good compromise between pilot symbol overhead and performance. For MIMO-OFDM channel estimation, however, the oversampling factor should be larger than two, to allow separation of the N_T antennas' signals. The overhead due to pilot symbols is $\eta = 1/(D_t D_f – 1)$, which should be kept as small as possible.

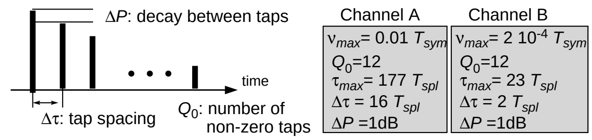

Fig. 4. The power delay profile of the used channel model.

TABLE I

OFDM SYSTEM PARAMETERS

Bandwidth	B	101.5 MHz
# subcarriers	N_c	769
FFT length	N_{FFT}	1024
Guard interval (GI) length	N_{GI}	226
Sample duration	T_{spl}	7.4 ns

TABLE II

CHANNEL ESTIMATION PARAMETERS

Parameter set	D_f	D_t	M_f	M_t	Δ_ℓ	η
(a.)	1	16	48	4	16	1/15
(b.)	2	8	32	6	16	1/15
(c.)	3	5	24	8	15	1/14
(d.)	4	4	16	10	16	1/15

IV. RESULTS

The MSE performance of the proposed 2×1D estimator is evaluted by using (13). The system parameters of the OFDM system were taken from [9], and are shown in Table I. The OFDM symbol duration with and without the guard interval is denoted by $T_{sym} = (N_{FFT} + N_{GI})T_{spl}$ and $T = N_{FFT}T_{spl}$, respectively; T_{spl} accounts for the sample duration. Two channel models were considered, one with large and one with small delay spread and Doppler frequency. The channel is modeled by a tap delay line model with $Q_0 = 12$ taps, a tap spacing of $\Delta\tau = 16 \cdot T_{spl}$ for channel A and $\Delta\tau = 2 \cdot T_{spl}$ for channel B, with an exponential decaying power delay profile, illustrated in Fig. 4. The independent fading taps are generated using Jakes model having a U-shape Doppler power spectrum [10]. The maximum Doppler frequency of each tap was set to $\nu_{max} = 0.01 \cdot T_{sym}$ for channel A and $\nu_{max} = 2 \cdot 10^{-4} T_{sym}$ for channel B, with T_{sym} defined in (2), corresponding to a mobile velocity of about 230 km/h and 5 km/h at 5 GHz carrier frequency, respectively. For the parameters of the robust channel estimator we assume knowledge about the maximum Doppler frequency and the maximum delay of the channel, so $\nu_{\max_w} = \nu_{max}$ and $\tau_{\max_w} = \tau_{max}$. The maximum expected SNR was set to $\gamma_w = 30$ dB.

In Fig. 5 the MSE performance is plotted for $N_T = 4$ transmit antennas, and different subset sizes N_{Tf}, by evaluating (13), and averaging over all ℓ and i. For the results plotted in Fig. 5, different parameter sets are compared, shown in Table II. Four different configurations of the pilot grid, D_f and D_t, are compared all having a similar overhead due to pilot symbols. The dimension of the Wiener filter in time direction, M_t, was selected such that the channel estimation delay and overhead due to pilots, Δ_ℓ and η, were comparable.

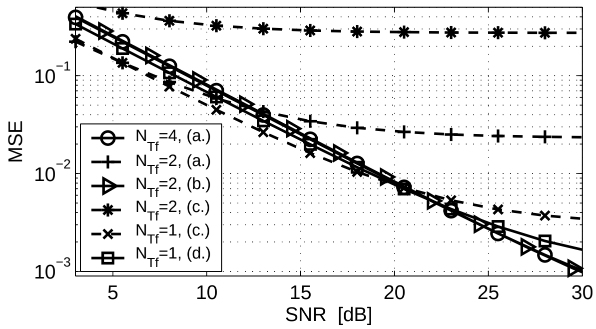

Fig. 5. MSE vs SNR for channel A, with different pilot spacings, D_f, D_t, and various subset sizes N_{Tf}, N_{Tt}. $N_T = 4$.

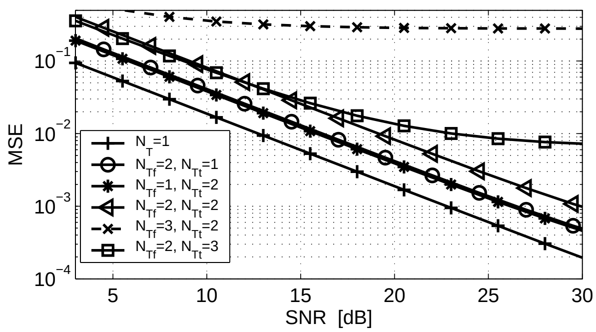

Fig. 6. MSE vs SNR for various antenna sizes $N_T = N_{Tf}N_{Tt}$, for channel A and parameter set (b.) from Table II.

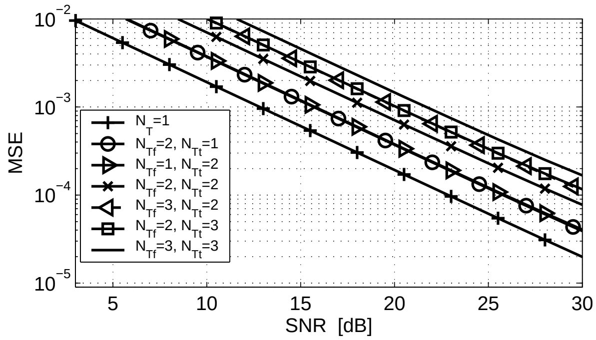

Fig. 7. MSE vs SNR for various antenna sizes $N_T = N_{Tf}N_{Tt}$, for channel B and parameter set (b.) from Table II.

Furthermore, M_f is chosen that the computational complexity of different parameter sets are comparable. For $N_{Tf} = 4$, all 4 transmit antennas' signals are separated in frequency direction. It is seen in Fig. 5 that the performance of a certain subset size N_{Tf} and N_{Tt} is closely related to a certain pilot spacing D_f and D_t, in the way that for increasing N_{Tf} and/or N_{Tt} the pilot spacing in that dimension must become denser, i.e. the oversampling rate is to be increased.

In Fig. 6 the MSE performance for various numbers of transmit antennas N_T is plotted against the SNR for parameter set (b.). It it not surprising to find that by increasing N_T the performance degrades. If the oversampling factor in frequency and time becomes smaller than N_{Tf} or N_{Tt}, the MSE is flatting out for high SNR.

Fig. 7 shows the MSE performance for the same parameters as the previous graph with channel B. For channel B the delay spread and the maximum Doppler frequency are smaller (see Fig. 4). This effectively increases the oversampling rate in frequency and time, and as a result the MSE performance improves and more transmit antennas N_T can be supported.

TABLE III

NUMBER OF MULTIPLICATIONS PER ESTIMATED CSI, $H_{\ell,i}^{(\mu)}$

N_T	N_{Tf}	N_{Tt}	D_f	D_t	M_f	M_t	$C^{[1]}$	$C^{[2]}$
1	1	1	2	8	32	6	28	134
4	4	1	1	16	48	4	20	194
	2	2	1	16	48	4	14	196
	2	2	2	8	32	6	20	131
	2	2	3	5	24	8	26	99
	1	4	3	5	24	8	21	102
	1	4	4	4	16	10	24	69
6	3	2	2	8	32	6	20	130
	2	3	2	8	32	6	17	131

The computational complexity of different parameter sets is shown in Table III. It is seen that for the chosen OFDM system parameters, performing channel estimation in frequency direction first is significantly less complex, $C^{[1]} \ll C^{[2]}$, for all considered parameters. The number of filter dimension in frequency is typically larger than in time, i.e. $M_f > M_t$. Moreover, provided that $D_f < D_t$, which is likely to be the case for the system parameters of Table I, then $C^{[1]} < C^{[2]}$.

V. CONCLUSIONS

In this paper we proposed a novel approach for MIMO-OFDM channel estimation in two dimensions. The channel estimation and separation task of the N_T superimposed signals were split using two cascaded one dimensional filters. The separation of superimposed signals ultimately requires a denser pilot spacing. By splitting the separation task into two stages, the 2×1D estimator can be adjusted to match a certain pilot grid, constraints on the filter dimensions in time and frequency, and other system parameters such as acceptable delay due to channel estimation in time direction. It was demonstrated that for the chosen OFDM system parameters performing channel estimation in frequency first is of advantage, due to the lower computational cost.

REFERENCES

[1] S. Weinstein and P. Ebert, "Data Transmission by Frequency Division Multiplexing Using the Discrete Fourier Transform," *IEEE Transactions on Communication Technology*, vol. COM-19, pp. 628–634, Oct. 1971.

[2] P. Hoeher, S. Kaiser, and P. Robertson, "Pilot-Symbol-Aided Channel Estimation in Time and Frequency," in *Proc. Communication Theory Mini-Conference (CTMC) within IEEE Global Telecommunications Conference (GLOBECOM'97), Phoenix, USA*, pp. 90–96, 1997.

[3] Y. Li, N. Seshadri, and S. Ariyavisitakul, "Channel Estimation for OFDM Systems with Transmitter Diversity in Mobile Wireless Channels," *IEEE Journal of Selected Areas on Communications*, vol. 17, pp. 461–470, Mar. 1999.

[4] Y. Li, "Simplified Channel Estimation for OFDM Systems with Multiple Transmit Antennas," *IEEE Transactions on Wireless Communications*, vol. 1, pp. 67–75, Jan. 2002.

[5] Y. Gong and K. Letaief, "Low Rank Channel Estimation for Space-Time Coded Wideband OFDM Systems," in *Proc. IEEE Vehicular Technology Conference (VTC'2001-Fall), Atlantic City, USA*, pp. 722–776, 2001.

[6] J. G. Proakis, *Digital Communications*. New York: McGraw-Hill, NY, USA, 3rd ed., 1995.

[7] J. K. Cavers, "An Analysis of Pilot Symbol Assisted Modulation for Rayleigh Fading Channels," *IEEE Transactions on Vehicular Technology*, vol. VT-40, pp. 686–693, Nov. 1991.

[8] S. M. Kay, *Fundamentals of Statistical Signal Processing: Estimation Theory*. Englewood Cliffs, NJ: Prentice Hall International, 1993.

[9] H. Atarashi, N. Maeda, S. Abeta, and M. Sawahashi, "Broadband Packet Wireless Access Based on VSF-OFCDM and MC/DS-CDMA," in *Proc. IEEE Intern. Symp. on Personal, Indoor and Mobile Radio Commun. (PIMRC 2003), Beijing, China*, pp. 992–996, Sep. 2002.

[10] W. C. Jakes, *Microwave Mobile Communications*. Wiley, NY, 1974.